Numerical optimization of grating-enhanced second-harmonic generation in optical waveguides

E. Popov

Laboratoire d'Optique Electromagnétique, Unité de Recherche Associée au Centre National de la Recherche Scientifique 843, Faculté des Sciences et Techniques de St Jérôme, 13397 Marseille Cedex 20, France, and Institute of Solid State Physics, 72 Tzarigradsko Chaussee, 1784 Sofia, Bulgaria

M. Neviere

Laboratoire d'Optique Electromagnétique, Unité de Recherche Associée au Centre National de la Recherche Scientifique 843, Faculté des Sciences et Techniques de St Jérôme, 13397 Marseille Cedex 20, France

G. Blau

Laboratoire d'Electromagnétisme, Microondes et Optoélectronique, Unité de Recherche Associée au Centre National de la Recherche Scientifique 833, Ecole Nationale Supérieure d'Electronique et de Radioélectricité de Grenoble, 23 Ave des Martyrs, B.P. 257, 38016 Grenoble Cedex, France

R. Reinisch

Laboratoire d'Electromagnétisme, Microondes et Optoélectronique, Unité de Recherche Associée au Centre National de la Recherche Scientifique 833, Ecole Nationale Supérieure d'Electronique et de Radioélectricité de Grenoble, 23 Ave des Martyrs, B.P. 257, 38016 Grenoble Cedex, France

Rigorous electromagnetic theory is combined with a phenomenological approach to permit optimization of grating-enhanced second-harmonic generation (SHG) in optical waveguides. Provided that the absorption losses in the optically nonlinear layer are not high, maximum SHG is observed when phase matching occurs between the incident wave at the pump frequency and guided waves at both the pump and the signal frequencies. Different coupling mechanisms are considered, and a procedure for determining the optimal groove depth and period of the grating is discussed. The phenomenological approach permits deeper physical insight into the problem and a considerable saving of computation time. Direct phase matching is shown to result in stronger SHG than indirect phase matching (performed through the grating vector), even if the former includes coupling between waveguide modes of different orders.   © 1995 Optical Society of America

1.   INTRODUCTION

Second-harmonic generation (SHG) in corrugated optical waveguides have attracted a great deal of interest.[1] It is expected that similar devices will perform many useful functions in optical signal processing[2,3]: light modulation, SHG, and optical logic. The guiding geometry is chosen because of its capability of concentrating energy.[4,5] Usually organic polymers are preferred as guiding layers because of their higher second-order susceptibility $\chi^{(2)}$ (Refs. 6–8) and better transparency in the visible and near-infrared regions. Their nonlinear properties seem to change by less than 10% over a duration of 5 years, they can endure high-power laser beams (up to 1 GW/cm²), and they can easily be spin coated. The most promising materials are currently obtained by copolymerization of a monomer (styrene, methylmetacrylate, or urethane). It would be desirable to generate green and blue light by doubling the frequency of near-infrared emitting diodes by utilizing the nonlinear properties of these layers and enhancing the light density through excitation of guided waves. The technical and economical consequences of

succeeding in this aim are obvious and explain the efforts made in many laboratories. It is strongly believed that phase matching between guided waves at the pump (ω_1) and signal (ω_2) circular frequencies (i.e., simultaneous mode excitation at ω_1 and ω_2) can sharply increase SHG as the result of electromagnetic field compression inside the guiding layer. In our previous paper[9] we showed that this is not always true: comparatively high absorption losses that could exist inside the optically nonlinear layer can drastically modify the system response so that instead of grating-enhanced SHG one can observe grating-reduced SHG.[10] In trying to avoid such cases it is important that one know what the optimum conditions are for obtaining maximum response. There are two possible directions for optimization: varying the groove parameters (profile form, depth, and period) or using different ways of phase matching among the incident, the radiated, and the guided waves. Carrying out such an investigation experimentally is a task of great difficulty that requires large amounts of time and funds. Fortunately, numerical modeling through rigorous methods can provide reliable information about the device's performance.

Such possibilities have been successfully exploited during the past two decades for the study of diffraction gratings in linear optics.

The main difficulty in optimizing corrugated waveguides in both linear and nonlinear optics comes from the great number of free parameters to be varied: groove form, depth, and period; waveguide optical index and thickness; substrate and cladding material. Our aim in writing this paper is to combine rigorous electromagnetic theory[11] with the phenomenological approach[12] to significantly reduce the number of these free parameters. Some reasonable assumptions concerning the system under investigation include utilization of a silver substrate and an organic nonlinear layer with fixed linear and nonlinear optical properties. For technological reasons the corrugation is introduced only at the lower boundary, and the upper waveguide–air interface is flat. Polarization is TM, with magnetic field parallel to the grooves, because spin-coated organic layers have anisotropic nonlinear susceptibility. Our aim was not to find an absolute maximum of SHG for a given device, a task that needs a much greater amount of research, but to try to find a procedure to search for a local maximum, thereby significantly reducing the computation time. To this aim we use a phenomenological approach,[13] well known in the linear grating studies. Section 2 presents a brief review of this approach as applied to SHG, together with the proper definitions. Sections 3 and 4 deal consecutively with direct and indirect phase matching to give numerical examples and to compare the magnitude of maximum SHG for several different cases.

2. PHENOMENOLOGICAL APPROACH TO GRATING-ENHANCED SECOND-HARMONIC GENERATION IN OPTICAL WAVEGUIDES

A plane wave with wavelength λ is incident from air at an angle θ_0 onto a thin layer, spin coated onto a silver grating so that the upper interface is flat and the lower one is corrugated (Fig. 1). This layer is thick enough to support waveguide modes, and it has nonlinear properties characterized by its second-order nonlinear susceptibility χ. It is assumed that the nonzero components of the third-rank tensor χ are $\chi_{xxy} = \chi_{xyx} = \epsilon_0$, $\chi_{yxx} = \epsilon_0$, and $\chi_{yyy} = 3\epsilon_0$, which correspond to polyurethane spin coated under a strong electric field upon a metallic grating, ϵ_0 being the vacuum permittivity. The incident wave is TM polarized, and its wavelength is 1 μm. The absorption losses inside the layer are low, the refractive indices at pump and signal frequency being

$$n_2(\omega_1) = 1.5785 + i4 \times 10^{-5},$$
$$n_2(\omega_2) = 1.6705 + i2.7 \times 10^{-5}.$$

The layer thickness is one of the free parameters to be varied, the others being the groove depth and the grating period. Depending on the period and the incident angle, single or several diffracted orders at ω_1 and ω_2 could propagate in the cladding; their number and direction are given by the grating equation

$$n_1(\omega_j)\sin \theta_{N_j}^{\omega_j} = n_1(\omega_1)\sin \theta_0 + N_j \frac{\lambda_j}{d}, \tag{1}$$

where the index $j = 1$ or 2, depending on the frequency, and $\theta_{N_j}^{\omega_j}$ is the angle of propagation of the Nth diffracted order. In what follows, $n_1(\omega_1) \equiv n_1(\omega_2) = 1$.

The conditions for excitation of a guided wave at ω_1 through the evanescent diffraction order with number N_1 are easily derived from Eq. (1):

$$\sin \theta_i \approx \mathrm{Re}(p_{m_1}^{\omega_1}) - N_1 \frac{\lambda_1}{d}, \tag{2}$$

where $p_{m_1}^{\omega_1}$ denotes the propagation constant of a mode with number m_1 and θ_i is the angle of incidence. It is well known that the amplitude of the guided wave a_{g_1} has a resonance at angle of incidence given by relation (2):

$$a_{g_1} = \frac{c_1}{\left(\sin \theta_0 - p_{m_1}^{\omega_1} + N_1 \dfrac{\lambda_1}{d}\right)}, \tag{3}$$

where c_1 is the incoupling coefficient, which depends on the geometrical and optical parameters of the system and $\theta_0 \equiv \theta_i$.

We are interested mainly in the case in which there is phase matching between a guided wave at ω_1 and another guided wave at ω_2. Then we can assume, at least in the phenomenological approach, that the main channel of coupling between the pump beam and the signal is between these phase-matched modes. Rigorous computations have proved this assumption,[12] at least within some limits discussed below with regard to the validity of Eq. (4). Then the nonlinear polarization term, which is proportional to the square of the electric field at ω_1, acts as a source of the waveguide mode at ω_2, the latter then being radiated in the cladding through diffraction order N_2. Taking all these considerations into account, we can express the amplitude a^{NL} of the propagation in the cladding diffraction orders at ω_2 in the form

$$a^{\mathrm{NL}} = a_{\mathrm{flat}}^{\mathrm{NL}}$$
$$+ \frac{c_1^2 J_{1-2} c_2}{\left(\sin \theta_0 - p_{m_1}^{\omega_1} + N_1 \dfrac{\lambda_1}{d}\right)^2 \left(\sin \theta_0 - p_{m_2}^{\omega_2} + N_2 \dfrac{\lambda_2}{d}\right)}, \tag{4}$$
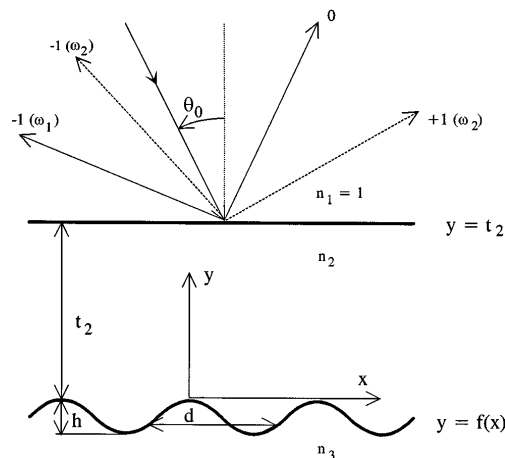
Fig. 1. Schematic of a layer with nonlinear properties, deposited upon a relief grating, together with the incident wave and the propagating diffracted orders at ω_1 and ω_2 in the cladding (air).

where c_2 is the outcoupling coefficient at ω_2 and J_{1-2}—the overlap integral between the two modes at ω_1 and ω_2. The first term, $a_{\text{flat}}^{\text{NL}}$, is the nonresonant part; for the specular reflected order it corresponds to the response of the system without corrugation.

Interpretation of Eq. (4) can easily be made from the point of view of the phenomenological theory of resonance anomalies in metallic gratings and corrugated waveguides: Simultaneous excitation of modes at pump and signal frequencies means that the amplitudes of the diffracted orders at ω_2 as a function of the angle of incidence have three poles: a double one, corresponding to the resonance at ω_1, and a single one, corresponding to the mode at ω_2, which immediately give rise to Eq. (4).

In fact, life is never so simple, and there are many cases in which the response is much more complicated. These cases include higher (but quite reasonable) losses inside the nonlinear layer or the metallic substrate.[9] Then the simple resonance behavior [second term of Eq. (4)] is complicated by the existence of complex zeros of the amplitudes. These zeros always accompany the poles, but for low-lossy structures their separation from the poles is usually larger than the imaginary part of the poles, so their influence on the resonance behavior is negligible. Otherwise, when the zeros are close to the poles, the resonances are much lower in amplitude and can even be transformed into dips.[9] As far as the aim of this paper is to optimize SHG, i.e., to search for maximal performance, we should try to avoid the influence of the zeros. In the examples chosen the complex zeros of the amplitudes lie outside the resonance domain. Of course, to check this we used a rigorous numerical method that makes no assumptions with regard to the position and the number of poles and zeros: the resonances appear automatically when Maxwell equations and boundary conditions are rigorously solved.

3. OPTIMIZATION ALGORITHM

After the optical properties of the media have been chosen, several degrees of freedom remain for optimization:

1. Depending on the thickness, the waveguide layer can support several modes at ω_1 and almost twice that number at ω_2, so phase matching between different modes can be used.

2. The phase matching can be direct, which means that the real parts of the mode propagation constants are equal:

$$\text{Re}(p_{m_1}^{\omega_1}) = \text{Re}(p_{m_2}^{\omega_2}), \qquad (5a)$$

or indirect, when the modes are coupled through, say, the Nth grating order:

$$\text{Re}(p_{m_1}^{\omega_1}) = \text{Re}(p_{m_2}^{\omega_2}) + N\,\frac{\lambda_2}{d}\,. \qquad (5b)$$

3. For a given type of mode coupling the amplitude of the SHG depends on the groove shape, period, and depth. The incoupling and outcoupling can be performed through either the first or higher diffraction orders, leading to a great variety in the amplitudes of the coupling coefficients c_1 and c_2.

In the first example we show the algorithm that is initially used for groove depth optimization. At first we consider direct coupling between the fundamental (first) mode at ω_1 and the second mode at ω_2. For this aim the dispersion characteristics of the planar (without corrugation) waveguide are drawn as a function of the middle layer thickness, so the desired thickness is chosen to correspond to the intersection point of the first mode at ω_1 and the second mode at ω_2. Then we determine the diffraction orders through which these modes are coupled in and out of the waveguide. For a shallow sinusoidal corrugation the coupling strength is closely proportional to h^N, where h is the groove depth and N is the number of the order in relation (2). Because of this power dependence it is better to use coupling through the 1st order, rather than through the higher ones, at least for shallow gratings. Numerical results confirm this conclusion, as shown below in Fig. 2. A change of the groove depth slightly modifies the mode propagation constants, so that for each given h it is necessary to determine $p^{\omega_1}(h)$ and $p^{\omega_2}(h)$, which one can do by using a numerical code for gratings in linear optics. Then it is necessary to modify the layer thickness t_2 slightly to fulfill the phase-matching conditions [Eq. 5(a)]. The angular dependence of the second-harmonic amplitudes of the propagating orders are obtained by use of a numerical code for nonlinear grating studies, and the maximum values are determined. Increase of the groove depth requires new mode determination, etc.

A typical example is presented in Fig. 2 of the interaction between the first mode at ω_1 and the second mode at ω_2. The initial layer thickness t_2 at $h = 0$ is 0.843 μm, and the grating period d is 0.47 μm. The real part of the mode propagation constants is 1.392, so under these conditions an angle of incidence $\theta_0 = -47.4°$ will correspond to mode excitation through the $+1$st diffraction order at ω_1. At ω_2 there are two diffraction orders that propagate in air: 0th and $+1$st (note that the angle of incidence is negative). The 0th order is coupled to the mode at ω_2 through two λ_2/d ratios, and the 1st order through only one, which explains the difference in their maximal amplitudes (Fig. 2).
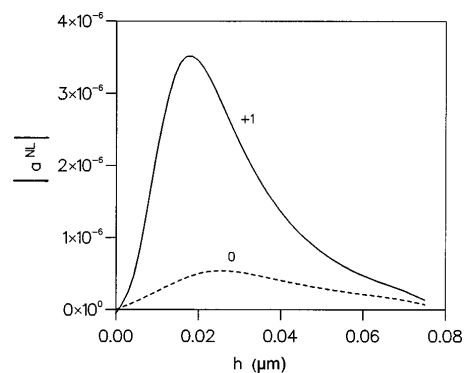
Fig. 2. Groove depth dependence of the absolute values of the amplitudes of the diffracted 0th (dashed curve) and $+1$st (solid curve) orders at ω_2 in the cladding. Sinusoidal grating with $d = 0.47$ μm, $n_2(\omega_1) = 1.5785 + i4 \times 10^{-5}$, $n_2(\omega_2) = 1.6705 + i2.7 \times 10^{-5}$, $n_3(\omega_1) = 0.129 + i6.83$, $n_3(\omega_2) = 0.05 + i2.87$, $t_2 = 0.838$ mm, $\lambda = 1$ μm, and TM polarization. Direct coupling 1–2 (i.e., between the first waveguide mode at ω_1 and the second one at ω_2).

The fact that maximal SHG is obtained at shallow corrugations enables us to extend the phenomenological approach further to save considerable computation time.

Let us return to Eq. (4). For a sinusoidal shallow grating several assumptions are valid:

1. The real part of the propagation constant of the modes does not change significantly with h, and the imaginary part grows as h^2. One can easily understand the latter dependence by taking into account that the sign of h plays no role in the radiations losses. Then

$$p_{m_j}^{\omega_j} \approx r_j + i(\delta_j + \gamma_j h^2), \qquad (6)$$

with $j = 1, 2$. This assumption can easily be proved by approximate theories, which are valid for shallow gratings. This means that the real part of p_m is practically independent of the groove depth and is equal to the real part r_j of the propagation constant for a plane waveguide and that the imaginary part grows as a square of the groove depth with the coefficient of proportionality γ_j. This dependence reflects the fact that the imaginary part of p_m does not depend on the sign of h. δ_j denotes the imaginary part of p_m at $h = 0$. Rigorous numerical confirmation is presented in Fig. 3 for the case given in Fig. 2.

2. The incoupling and outcoupling coefficients c_1 and c_2 are proportional to h^N:

$$c_j = \hat{c}_j h^{N_j}, \qquad j = 1, 2, \qquad (7)$$

where N_j is the number of the diffraction order that is responsible for the coupling [see relation (2)]. In the example presented in Fig. 2 the coupling at ω_1 is made through the 1st order. The coupling at ω_2 to the +1st order is also made through the 1st order, and the coupling to the 0th diffracted order through the 2nd order.

3. For the direct mode coupling ($r_1 = r_2$) the coupling (overlap) integral J_{1-2} does not depend on the groove depth. When the coupling is indirect, an assumption similar to Eq. (7) could be made for J:

$$J = \hat{J}h^N, \qquad (8)$$

where the direct coupling is included in Eq. (8) with $N = 0$.

4. If the groove shape is not sinusoidal, it is possible to make input and output coupling and mode coupling through higher Fourier harmonics of the profile. This possibility can easily be expressed in Eqs. (7) and (8) by substitution of the value of the amplitude of the Fourier harmonic responsible for the corresponding coupling for the groove depth h.

All these hypotheses can easily be checked numerically, as far as rigorous codes are available for both linear and nonlinear grating response. We stress the fact that, further on, assumptions 1–4 are used only to save computation time and facilitate optimization, the results always being compared with those obtained from the rigorous theory.

A. Simplest Case: Direct Coupling
Direct coupling was used when we plotted the +1st diffraction order at ω_2 in Fig. 2. We chose to couple

the incident wave to the first waveguide mode at ω_1 through the first evanescent order, as well as between the second mode at ω_2 and the radiated +1st order. The coupling between the modes is direct. All this enables us to write Eq. (4) in the following form:

$$\underset{\theta_i}{\mathrm{Max}} |a_{+1}^{\mathrm{NL}}(h)| = \left| a_{+1}^{\mathrm{NL}}(0) + i \frac{\hat{c}_1^2 \hat{c}_2 \hat{J} h^3}{(\delta_1 + \gamma_1 h^2)^2 (\delta_2 + \gamma_2 h^2)} \right|, \quad (9)$$

because $N_{1,2} = 1$ in Eq. (7), $N = 0$ in Eq. (8), Eq. (5a) is fulfilled ($r_1 = r_2$), and the maximum of $|a^{\mathrm{NL}}|$ as a function of θ_0 occurs when $\sin \theta_0 = r_1 - \lambda_1/d$. The flat case term in Eq. (9) is zero, but it is included there for generality.

The zero derivative with respect to h of Eq. (9) results in a doubly square equation for the groove depth h_{max} that corresponds to a local maximum of a^{NL}:

$$\gamma_1 \gamma_2 h^4 - \frac{h^2}{3}(\delta_1 \gamma_2 - \delta_2 \gamma_1) - \delta_1 \delta_2 = 0. \qquad (10)$$

It is interesting to note that Eq. (10) (and thus h_{max}) depends not on the coupling constants and the coupling integral but only on the initial losses of the modes without corrugation ($\delta_{1,2}$) and on the rate of the growth of radiation losses with groove depth ($\gamma_{1,2}$). This fact significantly facilitates the numerical optimization because it is necessary neither to calculate the coupling coefficients nor to have precise phase matching to determine h_{max} and $\mathrm{Max}_{\theta_0} |a^{\mathrm{NL}}(h_{\mathrm{max}})|$.

These results enable us to propose the following simple algorithm, summarized in Fig. 4:

1. At first the groove period d and the shape are chosen; then the layer thickness is determined to be close to the thickness required for direct phase matching between the modes at the two frequencies. Then mode propagation constants at $h = 0$ and at some small nonzero value h_s of h are obtained by one of the various numerical methods for gratings in linear optics. Then relation (6) is used to determine $\delta_{1,2}$, $\gamma_{1,2}$, and $r_{1,2}$. These values of r_1 and r_2
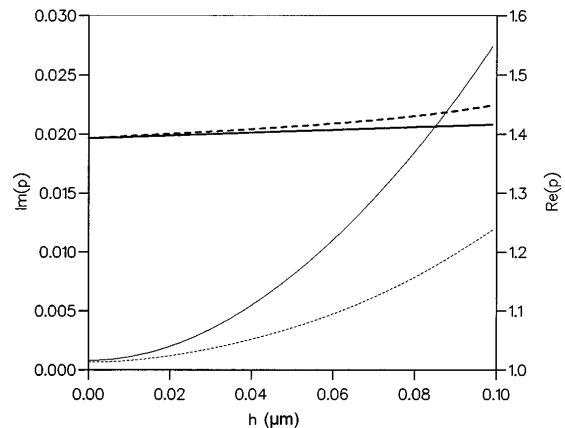
Fig. 3. Real (thick curves) and imaginary (thin curves) parts of the mode propagation constants at ω_1 (solid curves) and ω_2 (dashed curves) as a function of the groove depth, obtained by a rigorous electromagnetic theory. The parameters are the same as in Fig. 2.
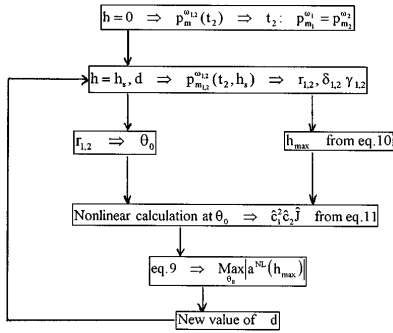
Fig. 4.   Flow chart of the optimization process.

are used to determine the angle of incidence that is close to the optimum one.

2.   One single calculation of the nonlinear grating response at that angle of incidence and $h = h_s$ enables the product of $\hat{c}_1^2 \hat{c}_2 \hat{J}$ to be determined by use of the more general form of Eq. (9), derived from Eq. (4):

$$a_{+1}^{\mathrm{NL}}(h_s) = \frac{\hat{c}_1^2 \hat{c}_2 \hat{J} h_s^3}{\left[\sin \theta_0 - r_1 + \dfrac{\lambda_1}{d} - i(\delta_1 + \gamma_1 h_s^2) \right]^2 \left[\sin \theta_0 - r_2 + \dfrac{2\lambda_2}{d} - i(\delta_2 + \gamma_2 h_s^2) \right]} \cdot \quad (11)$$

3. $h_{\max}$ is determined from Eq. (10) and then $\mathrm{Max}_{\theta_0} |a^{\mathrm{NL}}(h_{\max})|$ is determined from Eq. (9).

4.   The entire process is repeated as a function of the grating period, for different mode interactions, etc.   For several cases a full set of rigorous calculations of the true nonlinear response is made to check the results.   The rigorous calculations are made easier when the approximate value of $h_{\max}$ is known.

The validity of this approach is demonstrated in Fig. 5, which represents the dependence of $h_{\max}$ and $\mathrm{Max}_{\theta_0} |a^{\mathrm{NL}}(h_{\max})|$ as a function of the grating period for the same case as in Fig. 2.   The comparison between rigorous results (circles and asterisks) and the phenomenological algorithm (curves) shows very good agreement. The anomaly at $d = 0.74$ μm is due to a parasitic mode excitation at ω_2 and is discussed at the end of this section.

B.   Other Cases
The same approach can be applied for indirect coupling, coupling through higher diffraction orders, or high Fourier harmonics of the profile.   These possibilities have already been discussed with respect to Eqs. (5), (7), and (8).   A different value of the power dependence of h in the numerator of Eq. (9) [and Eq. (11)] will lead to another polynomial instead of to Eq. (10), but the optimization procedure based on these phenomenological equations will be the same as the one discussed in Subsection 3.A.

C.   Behavior of Coupling Coefficients
As we already discussed in Subsection 3.A, for the phenomenological optimization algorithm it is not necessary to know *a priori* the behavior of the coupling coefficients, except for some hypothesis on their groove depth dependence.   Of course, when rigorous nonlinear investigation is carried out, even this hypothesis is not required, but then the computation time grows significantly.

For physical insight, however, it is interesting to determine the dependence of the different terms in the numerator of Eq. (4), (9), or (11) on the grating and waveguide parameters.   This knowledge can be used successfully for the initial choice of the type of coupling between the incident and diffracted waves and waveguide modes. To this aim it is possible during step 1 in Subsection 3.A to determine $\hat{c}_{1,2}$ numerically by calculating the ratio between the incident wave amplitude and the evanescent order that corresponds to the excited waveguide mode. The mode overlap integral J cannot be obtained directly from the linear grating study, but it can be evaluated indirectly after the product $\hat{c}_1^2 \hat{c}_2 \hat{J}$ and the values of $\hat{c}_{1,2}$ are known.

In the case of direct mode coupling the overlap integral is almost independent of the grating parameters (groove form, depth, and period), at least for shallow grooves and far from the mode cutoff.   This can be intuitively expected and is confirmed by rigorous numerical study. Figure 6 presents the rigorous numerical results for the coupling coefficients $\hat{c}_{1,2}$ as well as for the entire coefficient $\hat{c}_1^2 \hat{c}_2 \hat{J}$ as a function of the groove period for the cases of Figs. 2, 3, and 5.   As can be expected, the period dependence $\hat{c}_1^2 \hat{c}_2 \hat{J}$ is completely determined by the dependence of the product of the incoupling and outcoupling coefficients $\hat{c}_1^2 \hat{c}_2$, pointing to the independence of the overlap integral.

The abrupt change of behavior of c_2 in Fig. 6(a) at $d \approx 1.3$ μm is due to the fact that for longer periods the +1st order at ω_2 does not propagate, i.e., this is a Rayleigh-type (passing-off) anomaly.   Of course, it can also be seen in the product $\hat{c}_1^2 \hat{c}_2$ and $\hat{c}_1^2 \hat{c}_2 \hat{J}$ in Fig. 6(b).

D.   Some Limitations and Precautions
The main limitations are due to the assumptions that led us to Eq. (4), relation (6), and Eqs. (7)–(11).   They are not valid when the groove depth increases, a fact that is
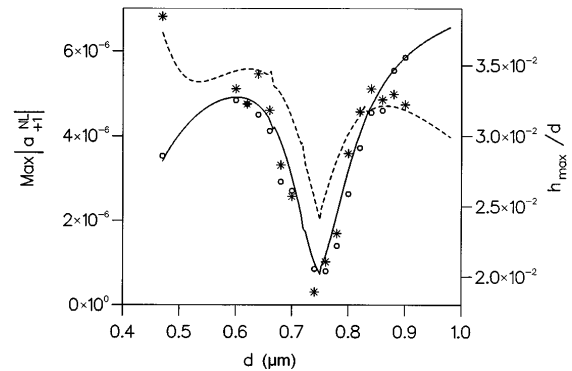
Fig. 5.   Maximum values of the amplitude $|a_{+1}^{\mathrm{NL}}|$ of the +1st diffracted cladding order (solid curve and circles) as a function of the grating period and the corresponding groove depth $h_{\max}$ (dashed curve and asterisks) at which these maxima occur.   The parameters are the same as in Fig. 2.   The curves are obtained according to the phenomenological approach, and the markers by rigorous theory.
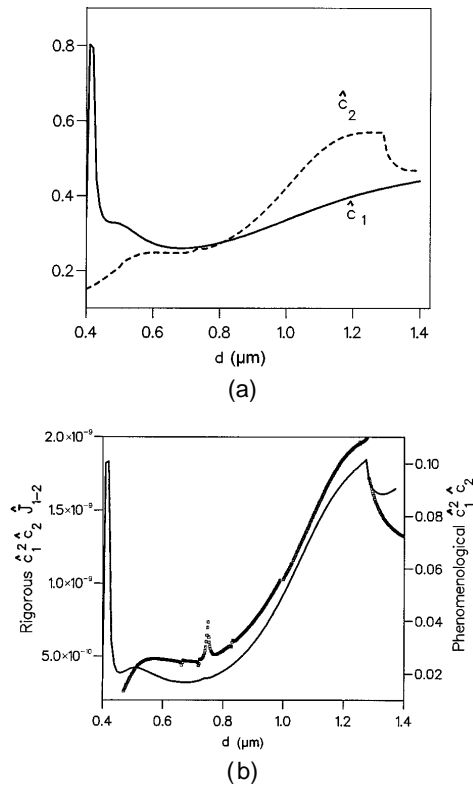
Fig. 6. (a) Input ($\hat{c}_1$) and output ($\hat{c}_2$) coupling coefficients calculated by a code for gratings in linear optics, corresponding to Figs. 2–4. (b) Comparison between the values of $\hat{c}_1^2\hat{c}_2\hat{J}_{1-2}$ (squares) as obtained by use of Eq. (10) and the rigorous results with the nonlinear code and the product $\hat{c}_1^2\hat{c}_2$, calculated from the data presented in (a) (solid curve).

well known in the linear optical study of gratings. Each case then requires rigorous numerical investigations.

The other obvious limitation occurs when several guided waves are simultaneously excited at ω_1 or ω_2. Then several different resonant terms must be introduced into Eqs. (4), (9), and (11), a fact also well known for gratings in linear optics. Because of the coupling between these multiple guided waves, however, the poles are repelled farther in the complex plane, so simple rules such as relation (6) and Eqs. (7) and (8) cannot be found. Moreover, because of this interaction the effective losses of the modes increase and the nonlinear effect decreases, as shown in Section 4. The conclusion is that parasitic mode excitation has to be avoided if large SHG is the object. As already mentioned, the dip near $d = 0.74$ μm in Fig. 5 is due to simultaneous excitation of two different waveguide modes at ω_2, which can easily be confirmed by the sharp maximum of the imaginary part of the mode propagation constant at ω_2 in Fig. 7. Interaction between different waveguide modes at the same frequency, which can easily be carried out by the grating under suitable phase matching, leads to an increase in the effective losses because of the energy transfer from one of the modes to the other.

4. NUMERICAL EXAMPLES

By varying the thickness of the waveguide it is possible to obtain direct coupling between the fundamental

mode at ω_1 and different modes at ω_2. A detailed analysis of the direct interaction of modes 1 and 2 has already been presented in Subsection 3.A. Because of the positive dispersion of the waveguide layer, it is not possible to have direct coupling between the fundamental modes (interaction of two modes 1) at the two frequencies, but for completeness we have investigated this case, choosing some arbitrary value of $n_2(\omega_2) = 1.56415$ greater than $n_2(\omega_1)$. Figures 8–11 correspond to Fig. 5, except that direct coupling between different modes is used. As it can be expected, the largest SHG is observed for coupling of two fundamental modes because of the largest overlap between the mode fields inside the optically nonlinear layer. Unfortunately, this case is almost impossible, because it requires negative dispersion.

As already discussed, the dip of the groove depth dependence for coupling of modes 1 and 2 is due to a parasitic mode excitation, so that SHG is higher for interaction of modes 1 and 3. This is also due to the larger overlap of mode 1 at ω_1 with mode 3 at ω_2 than with the second mode, the first two having almost symmetrical field maps and the last an antisymmetrical map.

The last example investigated covers the case of indirect coupling between the fundamental modes at the two frequencies. The media parameters are the same as in Figs. 2–7, except for the layer thickness $t = 1.88$ μm, which was chosen to be outside the region of parasitic mode excitations. To reduce the diffraction losses, there are no dispersive reflected orders at ω_1, which requires fine pitch grating. Choosing 0.47-μm groove spacing together with $t = 1.88$ μm ensures coupling between the fundamental modes at ω_1 and ω_2 propagating in opposite directions. A grating with a much larger period (e.g., $d = 2.28$ μm) can couple the fundamental modes propagating in parallel, but, mainly because of the great number of diffraction orders in the cladding at ω_1 and ω_2, the radiation losses become high so the system response at ω_2 is much weaker than for a fine pitch grating.

A sinusoidal grating can ensure backward mode coupling at ω_2 only through the third diffraction order (Fig. 12). If we go back to Eqs. (7)–(9), because of the first-order input and output coupling (Fig. 12) $N_{1,2} = 1$ in Eq. (7) but because of the third-order mode inter-
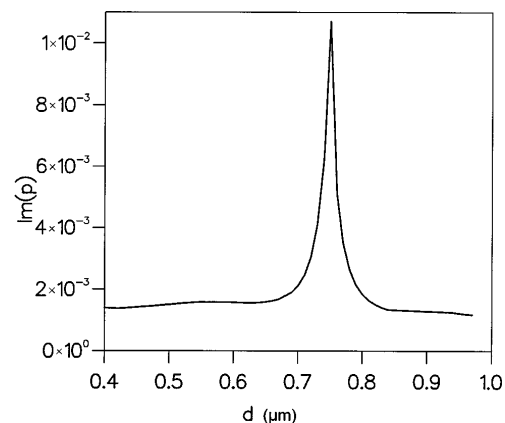
Fig. 7. Imaginary part of $p_2^{\omega_2}$ as a function of the grating period. The data correspond to those in Fig. 2, except for $h = 0.02$ μm.
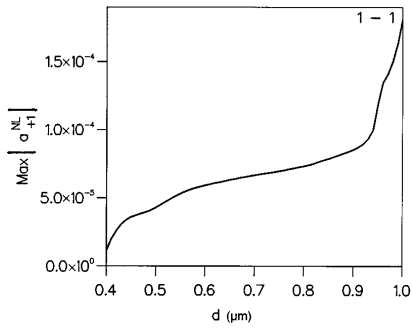
Fig. 8. Same as Fig. 4 except for the direct mode interaction 1–1. $n_2(\omega_2) = 1.56415 + i2.7 \times 10^{-5}$ and $t_2 = 1.505$ μm.
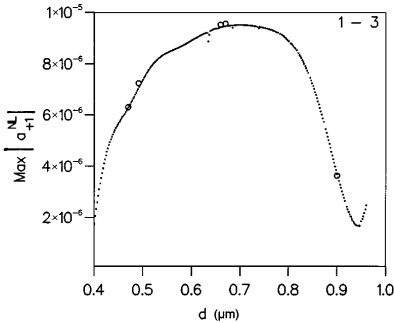
Fig. 9. Same as Fig. 4 except for the direct mode interaction 1–3. $t_2 = 1.513$ μm.
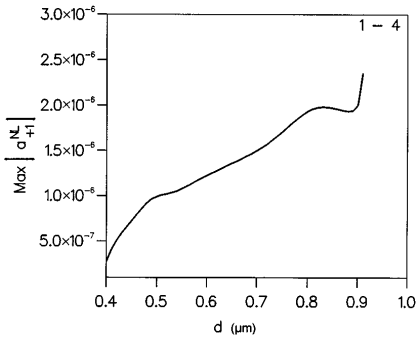
Fig. 10. Same as Fig. 4 except for the direct mode interaction 1–4. $t_2 = 2.066$ μm.
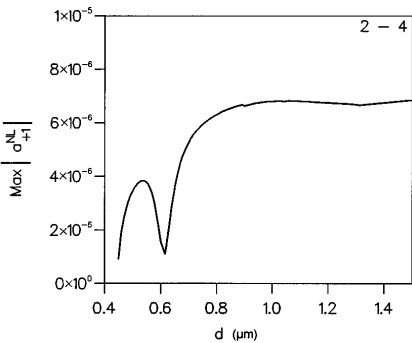
Fig. 11. Same as Fig. 4 except for the direct mode interaction 2–4. $t_2 = 1.13$ μm.

action $N = 3$ in Eq. (8), so the groove depth dependence of the numerator in Eq. (9) will be proportional to h^6 and the effect of SHG will become very weak

($a^{NL} < 10^{-8}$). That is why we have chosen a lamellar grating with a filling ratio 0.5, for which the ratio between the third (F_3^H) and the first (F_1^H) Fourier components of the profile function is highest (1/3) and there is no second-order Fourier component. Then the interaction between the fundamental modes carried out through the third Fourier harmonic is much stronger than through the third diffraction order of the first Fourier harmonic, the first being proportional to hF_3^H and the latter to $h^3F_1^H$.

With the lamellar profile, the numerator of Eq. (9) becomes proportional to h^4 so Eq. (10) takes a different form, and it predicts that a maximum of a^{NL} will occur at $h_{max} = 0.0318$ μm. This is fully confirmed by rigorous numerical study, and the result is $|a_0^{NL}| = 3.2 \times 10^{-7}$, much lower than in the case of a direct coupling. This can easily be explained by the stronger (magnitude 4) power dependence of the numerator of Eq. (9) on the groove depth for indirect coupling than for direct coupling and by the fact that maximal SHG is obtained for very shallow gratings.

It is impossible to vary the grating period independently as we have done for direct coupling, because indirect coupling is carried through the grating and, once the mode propagation constants are fixed by the layer thickness, their difference (or sum) determines the groove period. A typical angular dependence of the resonance curve for this case is presented in Fig. 13.
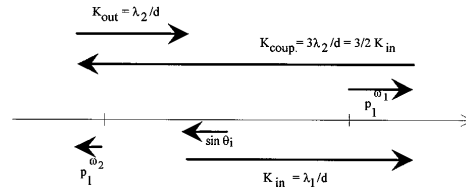
Fig. 12. Schematic representation of wave interaction in the indirect 1−1 coupling. The incident wave number (sin θ_i) is coupled through K_{in} to the mode at ω_1, which is then coupled to the mode at ω_2 through the third Fourier harmonic of the profile function K_{coup}. The mode at ω_2 is radiated through the first Fourier harmonic of the profile K_{out}.
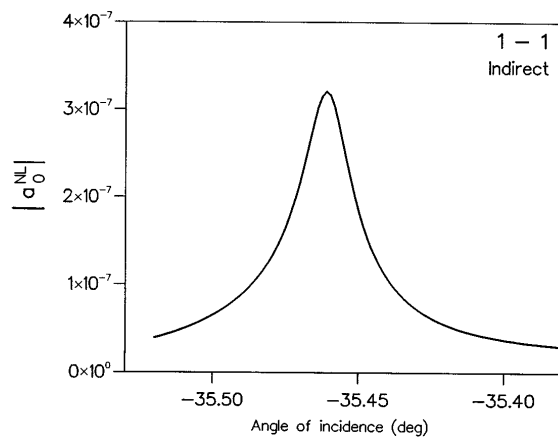
Fig. 13. Angular dependence of a_0^{NL}, corresponding to the coupling of Fig. 11. The refractive indices of the media are the same as in Fig. 2, $t_2 = 1.88$ μm, $d = 0.47$ μm, and the groove is characterized by two (1 and 3) Fourier harmonics with amplitudes $h_1 = 0.03183$ μm and $h_3 = h_1/3$.

5. CONCLUSION

A simple algorithm is proposed for numerical optimization of second-harmonic generation in corrugated waveguides. It combines the phenomenology of SHG based on the knowledge of complex poles of the scattering operator with the asymptotic low-modulation dependence of the input and output coupling coefficients and mode overlap integral. This algorithm is capable of dealing with direct and indirect phase matching and coupling through different diffraction orders and Fourier components with different profiles. A direct comparison with numerical results of a rigorous nonlinear study confirms its validity, at least for shallow corrugations.

The study shows that direct phase matching leads to a higher second-harmonic signal, even if it involves waveguide modes of different orders. For example, a waveguide with thickness 1.513 μm and sinusoidal corrugation with period 0.7 μm and groove depth 0.02 μm is able, at least theoretically, to achieve a diffracted wave at the second-harmonic frequency with an amplitude approaching 10^{-5} (Fig. 9). Given the experimentally available laser powers of approximately 40 kW over an area of 0.5 mm $\times$ 0.5 mm, the maximum conversion rate of 30% is found between the pump and the second-harmonic signal, which is most encouraging, considering that the device parameters have not been optimized with respect to the waveguide and substrate material properties.

However, this high efficiency value also points out the limits of the theories (e.g., Ref. 11) developed in the frame of the undepleted-pump approximation. At such high conversion factors the depletion of the pump should be included in the theory, which is much more difficult but is expected to give rise to cascading SHG, which lies outside the scope of this study but can lead to unexpectedly interesting behavior.[14]

ACKNOWLEDGMENT

REFERENCES

1. D. S. Chemla and J. Zyss, eds., *Nonlinear Optical Properties of Organic Molecules and Crystals* (Academic, New York, 1987), Vols. 1 and 2.
2. R. Ulrich, "Nonlinear optical organics and devices," in *Organic Materials for Nonlinear Optics,* R. A. Hann and D. Bloor, eds. (Royal Society of Chemistry, Cambridge, 1988), pp. 241–263.
3. T. K. Gaylord and M. G. Moharam, "Analysis and applications of optical diffraction by gratings," Proc. IEEE **73,** 894–937 (1985).
4. G. I. Stegeman, "Introduction to nonlinear guided wave optics," in *Guided Wave Nonlinear Optics,* D. B. Ostrowsky and R. Reinisch, eds. (Kluwer, Dordrecht, The Netherlands, 1992), pp. 11–27.
5. A. D. Boardman, K. Booth, and P. Egan, "Optical guided waves, linear and nonlinear surface plasmons," in *Guided Wave Nonlinear Optics,* D. B. Ostrowsky and R. Reinisch, eds. (Kluwer, Dordrecht, The Netherlands, 1992), pp. 201–230.
6. T. Kanetake, K. Ishikawa, T. Hasegawa, T. Koda, K. Takeda, M. Hasegawa, K. Kubodera, and M. Kobayashi, "Nonlinear optical properties of highly oriented polydiacetylene evaporated films," Appl. Phys. Lett. **54,** 2287–2295 (1989).
7. J. Messier, F. Kajzar, C. Sentein, M. Barzoukoz, J. Zyss, M. Blanchard-Desce, and J. M. Lehn, "Nonlinear optical susceptibilities of asymmetric push–pull polyenes," Nonlin. Opt. **2,** 53–62 (1992).
8. F. Kajzar, "Organic molecules for guided wave quadratic and cubic optics," in *Guided Wave Nonlinear Optics,* D. B. Ostrowsky and R. Reinisch, eds. (Kluwer, Dordrecht, The Netherlands, 1992), pp. 87–111.
9. E. Popov, M. Nevière, R. Reinisch, J.-L. Coutaz, and J. F. Roux, "Grating enhanced second harmonic generation in polymer waveguides: role of losses," Appl. Opt. **34,** 3398–3405 (1995).
10. M. Kull, J. L. Coutaz, and R. Meyrueix, "Experimental results of second harmonic generation from a polyurethane waveguide on grating coupler," Opt. Lett. **16,** 1930–1932 (1991).
11. E. Popov and M. Nevière, "Surface-enhanced second harmonic generation in nonlinear corrugated dielectrics: new theoretical approaches," J. Opt. Soc. Am. B **11,** 1555–1564 (1994).
12. M. Nevière, E. Popov, and R. Reinisch, "Electromagnetic resonances in linear and nonlinear optics: phenomenological study of grating behavior through the poles and the zeros of the scattering operator," J. Opt. Soc. Am. A **12,** 513–523 (1995).
13. M. Nevière, "The homogeneous problem," in *Electromagnetic Theory of Gratings,* R. Petit, ed. (Springer-Verlag, New York, 1980), Chap. 5.
14. R. Reinisch, "Bistabilité optique par génération de second harmonique sur des coupleurs à prisme ou à réseau," presented at the 14e Journées Nationales d'Optique guideé, October 25–26, 1994, Besançon, France.